

Position-Sensing Transition-Edge Sensors for Large-Field, High-Energy-Resolution X-ray Imaging Spectroscopy

Enectali Figueroa-Feliciano^{†,a,b}, Caroline K. Stahle^a, Fred M. Finkbeiner^{a,c},
Mary Li^{a,d}, Mark A. Lindeman^{a,e}, Nilesh Tralshawala^{a,d}, Carl M. Stahle^a

^aNASA Goddard Space Flight Center, Greenbelt, MD 20771 USA

^bStanford University, Department of Physics, Stanford, CA 94305 USA

^cUniversity of Maryland, Department of Astronomy, College Park, MD 20742 USA

^dRaytheon ITSS, Lanham, MD 20706 USA

^eNAS/NRC Resident Research Associate

ABSTRACT

In the X-ray astrophysics community, the desire for wide-field, high-resolution, X-ray imaging spectrometers has been growing for some time. We present a concept for such a detector called a Position-Sensing Transition-edge sensor (PoST). A PoST is a calorimeter consisting of two Transition-Edge Sensors (TESs) on the ends of a long absorber to do one dimensional imaging spectroscopy. Comparing the rise time and energy estimates obtained from each TES for a given event, the position of that event in the PoST is determined. Energy is inferred from the sum of the two signals on the TESs. We have designed 7, 15, and 32 pixel PoSTs using our Mo/Au TESs and bismuth absorbers. We discuss the theory, modeling, operation and readout of PoSTs and the latest results from our development.

Keywords: X-ray, calorimeter, microcalorimeter, spectrometer, imaging spectrometer, TES, PoST

1. INTRODUCTION

The X-ray sky offers some very interesting objects with enticing physics problems to be solved and phenomena to be understood over the next decade. Galaxy clusters, the intergalactic medium, active galactic nuclei and black holes, star clusters, X-ray binaries, super nova remnants, the diffuse X-ray background, stellar coronae, etc. will require ever increasing collection area and angular resolution from our telescopes and more increasingly stringent requirements from our detectors. Detector requirements are moving toward the perfect detector: high energy resolution, high quantum efficiency, high throughput, high timing resolution, large dynamic range, and large focal plane coverage. We want a detector that will do it all.

X-ray calorimeters, under development for the last 15 years, have shown great progress. Absorbers provide near perfect quantum efficiency with large packing fractions. Calorimeters have a large dynamic range, over one order of magnitude at X-ray energies. Sub 5 eV FWHM resolution at 6 keV has been achieved with TES calorimeters.¹ At X-ray energies, 100 μ s decay times for calorimetric pulses will provide rates of ~ 1000 counts per second per pixel. Current technology allows these time constants to be engineered into the design.

This leaves focal plane coverage. Because of the excellent optics available, which dictate small pixels for appropriate sampling of the point spread function (PSF), large focal plane coverage implies large number of pixels. The state of the art in calorimeters, XRS and the EBIT spectrometer,² have up to 32 pixels. Comparing this to large format X-ray CCD's with tens of megapixels, the need for new directions is clear. The reason for our current low number of pixels is number of available readout channels. There are several options being looked at for multiplexing readouts that will push calorimeters into the 1 kilopixel range needed for missions like Constellation-X.

We are developing an imaging calorimeter which uses transition-edge sensors on either side of a long absorber to read out tens of pixels with two channels. We call this device a Position-Sensing TES (PoST). Timing and energy differences in the pulses on each TES for a given X-ray event are used to determine its position. In this way, we

[†]Correspondence address: Laboratory for High Energy Astrophysics, NASA Goddard Space Flight Center, Mail code 662, Greenbelt, MD, 20771, USA Tel: 301-286-1249 Fax: 301-286-1684 E-mail address: Enectali.figueroa@gsfc.nasa.gov

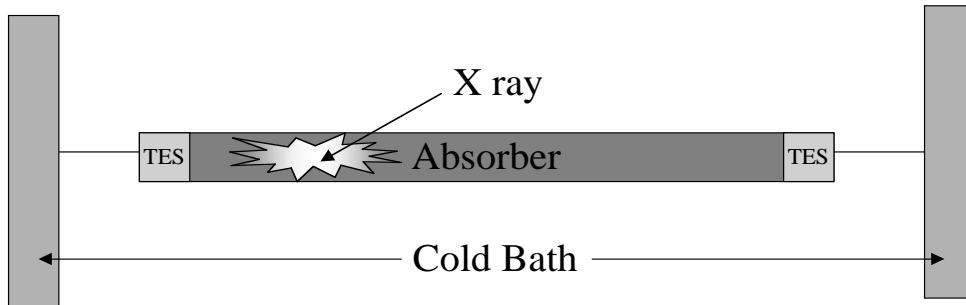


Figure 1. Concept for one-dimensional PoST imaging calorimeter. Two thermometers sense the same event, and the difference in signals provides the position information, while the pulse heights provide a measurement of the energy.

increase the number of pixels by an order of magnitude or more for a given number of channels. Coupled to readout multiplexing technologies, we can increase our pixel count to the tens of kilopixel range, where we can begin to consider large field of view applications.

2. IMAGING CALORIMETER BASICS

A calorimeter consists of an absorber connected to an energy reservoir and instrumented with a thermometer. When an absorption event occurs, the energy transferred to the absorber from the incident particle causes an increase in temperature which is measured by the thermometer. Since the absorber is connected to an energy reservoir, the absorber returns to its quiescent temperature. Because the increase in temperature is proportional to the energy deposited by the particle, this energy can be determined from the thermometer signal. In our case, the particles are photons, but they could be anything from molecules to neutrinos.

In general, an imaging calorimeter uses one or more thermometers to analyze the signal produced by a photon absorption event in an absorber. For the same energy photons, the signal received by the thermometers varies in some detectable way depending on the position in the absorber where the event occurred. In other words, the absorber exhibits position dependence. If one can use the information in the signal shape to determine the location of photon absorption and the photon energy, one has an imaging calorimeter. This definition does not impose restrictions on the type of thermometer or absorber used, nor on the method of position or energy determination from the produced signal. For this paper, we will concentrate on a one-dimensional imaging calorimeter design using two TES thermometers flanking an X-ray opaque absorber. A schematic of the concept is shown in Figure 1. The width of the PoST defines the pixel size in that direction, while the length-wise pixel size depends on how one bins the information from the detector and depends on the application. For Constellation-X detectors, the pixel size needed to sample the PSF is around $250 \mu\text{m}$, so this would be the width of the PoST, while the number of pixels would be equal to the length of the absorber divided by $250 \mu\text{m}$. When an X-ray event occurs, heat propagates down the absorber and reaches the thermometers. Since the PoST is connected to a cold heat sink, after the initial heating from the X-ray event it returns to its quiescent state. The timing, pulse height, and rise time of the pulse on each TES will depend on the absorption location (Figure 2).

3. POST DESIGN CONSIDERATIONS

On studying the idea of using imaging calorimeters, there are two issues to consider when comparing them to single pixel calorimeters: count rate and energy resolution.

3.1. Count rate

In general, PoSTs use each channel in a calorimeter to read out several pixels. This channel multiplexing must come at a price. To compare to a single channel calorimeter, we must define maximum count rate. By maximum count rate we mean the counts per second the calorimeter can absorb and still have only one pulse per digitized trace. This rate will depend on the decay time of the pulse, called the effective time constant, τ_{eff} .

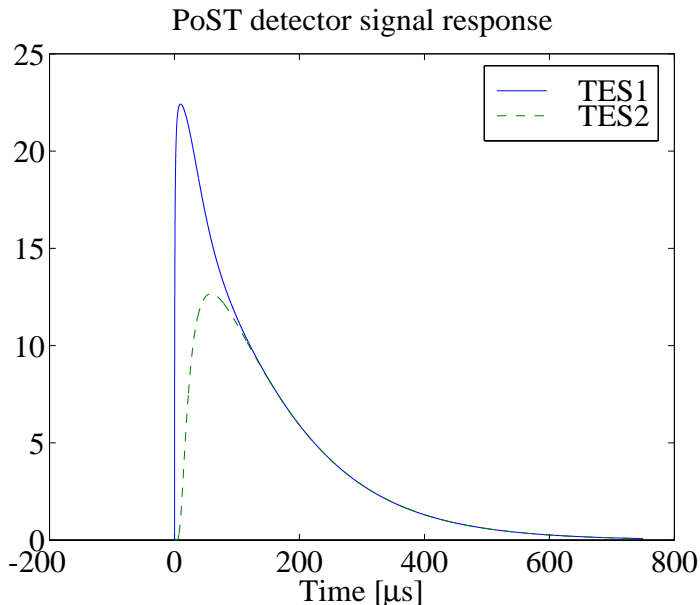


Figure 2. Response of a PoST to a photon absorption event. From the difference in pulse heights, the position of the event can be determined.

If the τ_{eff} for the PoST is the same as for a single pixel TES, then the maximum count rate will go down as the number of pixels in the PoST increases. If the τ_{eff} is longer than the single pixel calorimeter, then the rate will go down further by a factor proportional to the ratios of the time constants. The important question is whether the maximum count rate goes down linearly with the number of pixels in the PoST. At first glance the answer is yes. If a single pixel TES can handle 1000 counts per second, then a PoST, with two TESs and 30 pixels will be able to see 1000 counts per second. Each pixel would only handle 33 counts per second, as long as the counts are distributed evenly among the pixels. That sounds very discouraging. But herein lies the catch. When looking at astrophysical sources, most objects that produce 1000 counts per second per pixel are point sources. If we oversample the PSF of the telescope by a factor of three, the high count rate is seen by only three of the pixels in one PoST. The other 27 pixels see much reduced count rates. In other words, although the maximum rate is still 1000 counts per second, we would be able to look at sources that are around 300 counts per second whether the PoST has 10 pixels or 30. Then the question becomes whether an increase in field of view of 15 is worth a cut in throughput by a factor of 3.5.

As a final note on this point, our design is completely compatible with the single pixel TES processing. There is no reason why a viable flight instrument could not have a 6×6 single pixel array surrounded by PoSTs. The single pixel array would then handle the 1000 count per second objects, and extended objects would be imaged by the complete instrument. If 1000 readout channels are available, using 36 for single pixels still provides with 964 for PoSTs. For 30 pixel PoSTs, at 15 pixels per channel, that would add up to a 14,500 pixel instrument, compared to a 1000 pixel instrument without PoST technology.

3.2. Energy resolution

Energy resolution is the most important concern when designing a PoST. No matter what the increase in field of view, the instrument is still first and foremost a spectrometer. Let's look at how using two thermometers affects resolution. Consider a single pixel device that is $400 \mu\text{m}$ to a side. It has an absorber and is suspended on silicon nitride to provide the thermal decoupling from the substrate. Now suppose we split this TES in two, creating two thermometers that are $200 \mu\text{m}$ wide and $400 \mu\text{m}$ long. The power required to keep the TESs in their biased position is still the same, so each half must contribute $P_o/2$, where P_o was the original quiescent power dissipated in the TES. The total heat capacity is the same, and the thermal conductance to the reservoir is the same (since all we have done is slice the TES). This all implies that the pulse shape will be unaffected by our use of two thermometers. The signal obtained from each detector will be identical to that from the other. If the bias rails on the split detector are placed so that each TES has half the resistance of the original square, then by adding the signals together, we

regain the original pulse height. Now what happens to the noise? Will the noise in the two signals be correlated or uncorrelated? The answer is frequency dependent. The original TES had a thermalization time τ_{th} related to the resistance of the TES by the Wiedemann-Franz law. This thermalization time gives the time constant of heat moving from one side of the TES to the other. The fact that the TES is split in two makes no difference in this τ_{th} . For frequencies below $1/\tau_{th}$, phonon noise (which is a local excess or loss of energy) can equilibrate from one side to the other, and thus at these frequencies the phonon noise seen by the two TESs will be correlated. At frequencies much higher than $1/\tau_{th}$, phonon noise on one side does not have time to travel from one TES to the other, and at these frequencies the TESs act as if they were thermally decoupled. Thus the phonon noise will be uncorrelated. This happens at high frequencies which are out of the signal band; for resolution purposes the noise can be treated as correlated and thus simply adds. The result, as one might have guessed, is that splitting one TES in two and reading the halves out separately does not degrade resolution. You get back exactly the same signal. In fact, other sources of noise, such as amplifier noise, do add in quadrature and are thus $\sqrt{2}$ less than in the single TES case.

The energy resolution of a calorimeter is proportional to the square root of the heat capacity ($\Delta E \propto \sqrt{C}$).³ So if we want to make a PoST with the same energy resolution as our example above, our total heat capacity (2 TESs plus absorber) must equal that of the single pixel TES. This has certain implications. If one makes the absorber thermalize fast enough, so that τ_{th} is much smaller than the decay time τ_{eff} of the PoST, i.e. $\tau_{th} \ll \tau_{eff}$, then the whole PoST will act as one TES, and the energy resolution will be the same as for the single pixel. The price we pay is in position resolution. Since one needs the τ_{th} to be small, it will be difficult to determine the position of the event, since both TESs will have almost the same shape and amplitude pulse. So by increasing the τ_{th} from its single pixel value just enough to get the minimum position resolution we desire, we maximize our energy resolution. This intuitive result can be restated as follows. The more the two pulses are alike, the better the energy resolution we can get. The more the pulses are different from each other, the better the position resolution we can get. Since we are looking for a part in 3000 energy resolution and a part in 30 position resolution, it makes sense to design for very fast thermalization. To quantify the degradation in energy resolution for a particular amount of position resolution requires the derivation of an analytical model for PoST detectors from which theoretical noise can be calculated. We are currently in the process of developing such a theory, and will publish our findings on a forthcoming paper.

As one makes the PoST longer, the thermalization time will increase. At some point, the thermal conductance between the two TESs is so small they no longer act as a single unit. In this regime, an X-ray that lands next to one of the TES will be mostly sensed by that TES, and the other TES will be almost oblivious to the photon. Here each TES must be able to act as a single pixel device, and thus needs the same heat capacity as a single device. To avoid saturating the TESs in the PoST, the total heat capacity of the PoST will need to be twice as big as the single pixel TES, and the resolution will degrade by a factor of $\sqrt{2}$ from the increase in heat capacity. The impact on energy resolution from having a small thermal conductance (large τ_{th}) between the two TES is currently under study.

There are other factors which will probably make the PoST resolution lower than in the ideal-case discussed above. One such possibility is in analysis. Optimal filtering of a continuously varying pulse shape is a challenge. We have been developing analysis methods to get the best possible resolution from varying pulse shapes.⁴

4. GODDARD MO/AU POSTS

In this section we discuss some of the particular design and fabrication issues as well as describe the different components of a PoST imaging calorimeter.

4.1. Transition-edge sensors

We are working with resistive thermometers – specifically Transition-Edge Sensors. A TES is a superconducting thermometer biased in its superconducting transition. Small temperature changes produce large changes in resistance, providing excellent thermometric sensitivity.

The overall performance of PoSTs obviously depends on the TESs used for its readout. Here we give a brief summary of our single pixel calorimeter development. For a more detailed description, please see the paper by Stahle in these proceedings.⁵

We are developing single pixel TESs using Mo/Au bilayers, with tuned transition temperatures of 100 mK. We have fabricated TESs ranging from $150\ \mu\text{m}$ to $600\ \mu\text{m}$ to a side. The TES is suspended in a silicon nitride membrane for thermal decoupling, and we have recently begun using a postage-stamp style slitting to reduce the area required

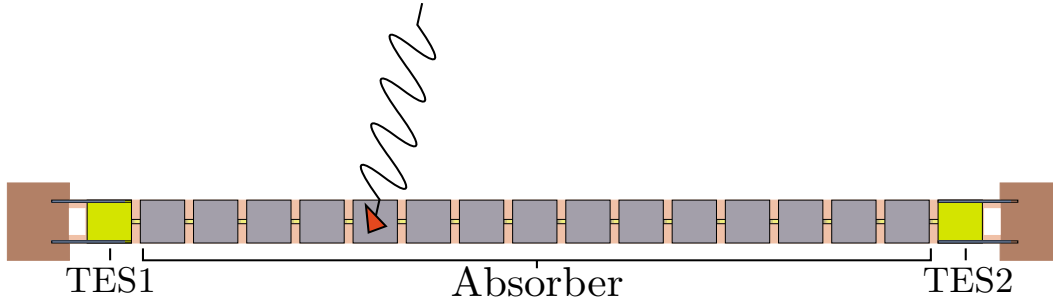


Figure 3. Goddard PoST concept. Mo/Au TESs on either side of a bismuth absorber sense the signal. The bismuth is pixellated to make it easier to determine the position of the event.

by the nitride to achieve the appropriate conductance. The TES resistance is $10 \text{ m}\Omega/\square$. These devices exhibit sub-millikelvin transitions, and we have demonstrated resolutions of $2.8 \text{ eV FWHM @ } 1.5 \text{ keV}$ and $3.7 \text{ eV FWHM @ } 3.3 \text{ keV}$.⁶

4.2. Absorbers

Absorbers are also a very important aspect of the PoST design, and our bismuth absorber technology has proven very useful. Bismuth offers the large stopping power and low heat capacity desired for absorber materials. It is also fully compatible with our integrated fabrication procedure. In order to obtain high packing fractions, we have successfully fabricated 3-dimensional Bi structures (called mushrooms) where there is a base which touches the substrate (which we call the stem), and an overhang that protrudes from this base for distances of up to hundreds of microns. The space between the substrate and the overhang is $\sim 1 \mu\text{m}$. This mushroom structure allows for wiring and nitride area on the perimeter of the TES while allowing the absorbers to come to within several microns of each other, producing an excellent packing fraction. 32×32 arrays of these absorbers have been fabricated on silicon substrate, and we are in the process of fabricating TES calorimeter arrays with these absorbers.

The one drawback to bismuth for PoST purposes is that, as a semi-metal, its thermal conductivity is very low. The desired conductances for our design were much faster than that of Bi. To achieve these conductances, we added a gold thermalization layer between the nitride and the Bi. The gold acts as a thermal short and allows us to engineer the conductance of the thermal link to make the appropriate thermal connection between the two TESs.

Since determining the position of an absorption event is paramount to the success of a PoST, we have integrated the position sensing into the design by pixellating the absorber. Figures 3 and 4 illustrate the concept. The bismuth is deposited in square mushrooms which are $150 \mu\text{m}$ long at the stem and $250 \mu\text{m}$ long at the top. Placed end to end, this leaves $100 \mu\text{m}$ of space between adjacent mushroom stems. The gold thermal short is $250 \mu\text{m}$ wide under the stem, but $\sim 10 \mu\text{m}$ wide between stems. The gold layer acts as the main pixellation mechanism. Gold covers all the Bi stem area, so X-rays thermalize quickly in the pixel, no matter where the incident X-ray hit. Between pixels, however, the narrow gold provides controlled heat transfer at whatever rate we desire. Modeling these devices using a finite-element method provided us with appropriate values for these thermal links. We chose links that were $100 \mu\text{m}$ long, 247 nm thick, and from 5 to $15 \mu\text{m}$ wide. These are calculated to provide pixel to pixel conductivities of $\sim 10 \text{ nW/K}$.

The effect of pixellation in the absorber is to greatly simplify the data processing for the PoST. Without a pixellated absorber, each position in the absorber will produce a slightly different pulse on each TES. We would have to then bin the pulses together to create “pixels.” However, within each “pixel” pulse variations would still exist, potentially degrading the resolution. Since the pixels have a very small internal thermalization time, no matter where in the pixel the X ray gets absorbed, the whole pixel will rapidly thermalize, and heat will flow out of it through the gold thermal links to the adjacent pixels. These in turn will heat rapidly as a unit and so on down the absorber until the TESs are reached. By alternating areas of very high thermal conductivity (under the absorber stems) and areas of moderate thermal conductivity (the inter-stem links) we have parceled the position dependence into discrete elements. Distinguishing these discrete elements from one another is much easier than looking at events from a solid absorber with a constant thermal conductance across it. From our models the inter-pixel conductances

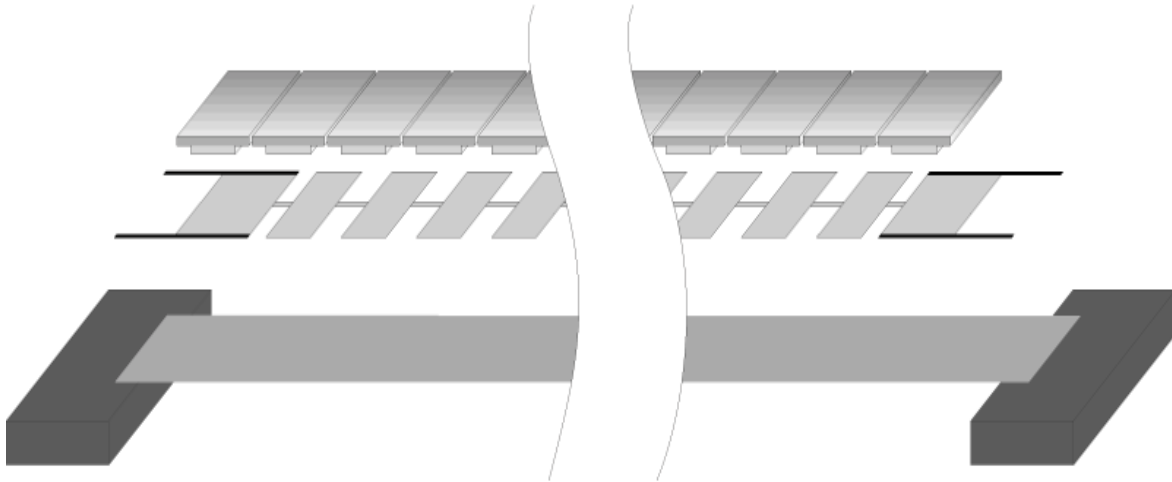


Figure 4. Expanded view for one-dimensional PoST imaging calorimeter. At the top the bismuth mushrooms are seen. Next comes the gold thermal conductance bridge flanked by the two Mo/Au TESs. Finally the silicon-nitride bridge, which provides the thermal decoupling of the detector from the cold bath, as well as structural support to the absorber.

of ~ 10 nW/K are high enough to make the response of the PoST fast, but slow enough to clearly distinguish the pixel that was hit.

4.3. Nitride

As described above, the desire is for the PoST to act as much as possible as a single pixel. This means that the thermalization time of the whole PoST must be small compared to the pulse decay time constant τ_{eff} . Using gold allows the inter-pixel conductivities to be very high, providing the small thermalization times. The whole PoST is deposited on a $0.5 \mu\text{m}$ thick silicon nitride bridge. Along the PoST, the contributions of the nitride to heat capacity and thermal conductivity are negligible; it only acts as a structural element. On the ends, however, it acts as the thermal bottleneck from the PoST to the substrate. To be conservative on our first devices, we designed the conductance of the silicon nitride connecting the PoST to the cold bath to be ~ 10 pW, 1000 times lower than the pixel to pixel conductance.

4.4. Mechanical Models

The mechanical behavior of these devices remains to be modeled. We will begin constructing a mechanical model of a PoST in the coming weeks to determine the lowest frequency of oscillations, which we wish to keep well above our bandpass. If this frequency lies inside our bandpass, susceptibility to microphonic pickup in the devices will be an issue.

4.5. Fabrication and Testing

The fabrication of PoSTs is fully compatible with our current fabrication process for the single TES devices. A description of our fabrication process can be found in Ref. 7. We are fabricating the first Mo/Au PoST devices and will begin testing soon. The long silicon-nitride bridges (which were a point of worry since we had never fabricated such long silicon-nitride structures) have held up well to processing. All other steps are from our standard process and should pose no problems.



Figure 5. Schematic of a 900 channel, 900 pixel imaging calorimeter using single pixel TESs.

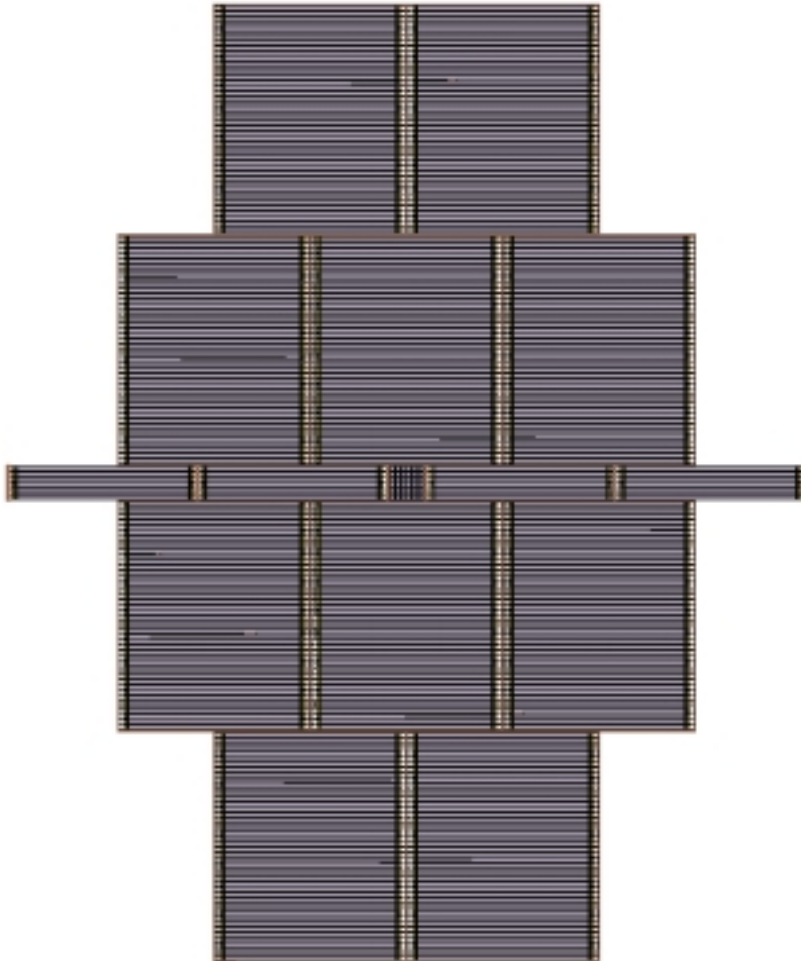


Figure 6. Schematic of a 900 channel, 13000 pixel imaging calorimeter using a 6×6 single pixel core surrounded by PoST detectors. This image and Figure 5 are in the same scale.

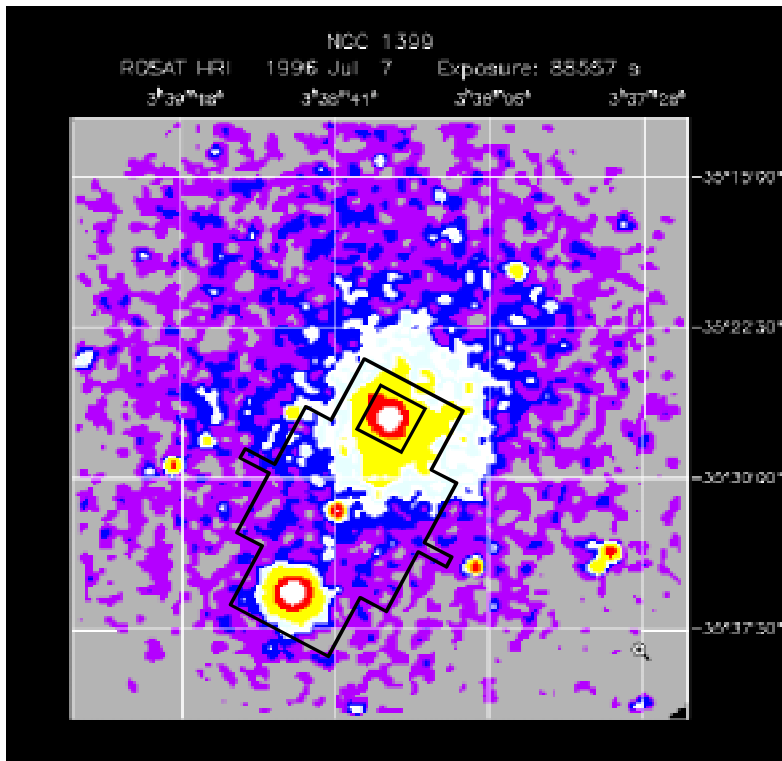


Figure 7. Galaxy group NGC1399. The outlines show the focal plane coverage using 10-meter-focal-length X-ray optics and the two detectors in the previous figures.

5. CONCLUSIONS: A PREVIEW OF THINGS TO COME

Although much remains to be done, PoSTs will be tested and first results obtained in the very near future. We have presented the foundations of our PoST design and discussed the position and energy resolution issues that will ultimately be the drivers of PoST design parameters. To illustrate the power of an order and a half of magnitude increase in focal plane coverage provided by our PoST design, we present the following images of a hypothetical hybrid calorimeter consisting of a 6×6 single pixel array surrounded by 432 PoST detectors. Figure 5 shows the focal plane coverage obtained by a 900 channel system using single pixel TES calorimeters. In Figure 6, the hybrid detector is shown to scale. The irregular shape is not necessary; it is just an artifact of the method use to put together this schematic for illustration purposes. The much larger coverage is evident. In Figure 7, we show a ROSAT image of the galaxy group NGC1399. The PSF of ROSAT is similar to what is expected from Constellation-X optics. The two thick outlines are the portions of the sky that the two detectors on the previous figures would see if looking through a telescope similar to that of Constellation-X. The advantages of kilopixel arrays are self evident.

ACKNOWLEDGMENTS

We would like to thank Blas Cabrera, John Mather and Harvey Moseley for useful discussions.

REFERENCES

1. K. D. Irwin, G. C. Hilton, H. M. Martinis, S. Deiker, N. Bergren, S. W. Nam, D. A. Rudman, and D. A. Wollman, "A Mo-Cu superconducting transition-edge microcalorimeter with 4.5 eV energy resolution at 6 keV," *Nucl. Inst. and Meth. A* **444**, pp. 184–187, 2000.

2. S. F. Porter, M. D. Audley, P. Beiersdorfer, K. R. Boyce, R. P. Brekosky, G. V. Brown, K. C. Gendreau, J. Gygas, S. Kahn, R. L. Kelley, C. K. Stahle, and A. e. Szymkowiak, "Laboratory astrophysics using a spare XRS microcalorimeter," *in these proceedings* .
3. S. H. Moseley, J. C. Mather, and D. McCammon, "Thermal detectors as X-ray spectrometers," *J. Appl. Phys.* **56**, pp. 1257–1262, 1984.
4. E. Figueroa-Feliciano, B. Cabrera, A. J. Miller, S. F. Powell, T. Saab, and A. B. C. Walker, "Optimal filter analysis of energy-dependent pulse shapes and its application to TES detectors," *Nucl. Inst. and Meth. A* **444**, pp. 453–456, 2000.
5. C. Stahle, R. P. Brekosky, E. Figueroa-Feliciano, F. M. Finkbeiner, J. D. Gygas, M. Li, M. A. Lindeman, F. S. Porter, and N. Tralshawala, "Progress in the development of Mo/Au transition-edge sensors for X-ray spectroscopy," *in these proceedings* .
6. E. Figueroa-Feliciano, C. K. Stahle, F. M. Finkbeiner, R. Kelley, M. A. Lindeman, F. S. Porter, N. Tralshawala, M. Li, and C. M. Stahle, "Mo/Au TES X-ray calorimeter with 2.8 eV resolution at 1.5 keV," *Proc. X-ray to X-band: Space Astrophysics Detectors and Detector Technology Workshop* , 26 to 29 June 2000.
7. N. Tralshawala, M. Li, C. M. Stahle, R. Brekosky, E. Figueroa-Feliciano, F. M. Finkbeiner, and C. K. Stahle, "Development of close-packed microcalorimeter arrays using molybdenum-gold transition-edge sensors with bismuth absorbers," *Proc. X-ray to X-band: Space Astrophysics Detectors and Detector Technology Workshop* , 26 to 29 June 2000.